Reflection infrared spectroscopy for the non-invasive in situ study of artists' pigments

ARTICLE *in* APPLIED PHYSICS A · OCTOBER 2012

Impact Factor: 1.7 · DOI: 10.1007/s00339-011-6708-2

4 AUTHORS:

Costanza Miliani
Italian National Research Council
130 PUBLICATIONS **1,554** CITATIONS
SEE PROFILE

Francesca Rosi
Italian National Research Council
43 PUBLICATIONS **509** CITATIONS
SEE PROFILE

Alessia Daveri
Associazione Laboratorio di Diagnostica pe…
14 PUBLICATIONS **163** CITATIONS
SEE PROFILE

Bruno Brunetti
Università degli Studi di Perugia
169 PUBLICATIONS **1,879** CITATIONS
SEE PROFILE

Appl Phys A (2012) 106:295–307
DOI 10.1007/s00339-011-6708-2

Applied Physics A
Materials Science & Processing

INVITED PAPER

Reflection infrared spectroscopy for the non-invasive in situ study of artists' pigments

C. Miliani · F. Rosi · A. Daveri · B.G. Brunetti

Received: 13 April 2011 / Accepted: 7 November 2011 / Published online: 21 December 2011

Abstract The potential of fibre optic reflection infrared spectroscopy for the non-invasive identification of artists' pigments is presented. Sixteen different carbonate, sulphate and silicate-based pigments are taken into account considering their wide use during the history of art and their infrared optical properties. The infrared distortions mainly generated by the specular reflection are discussed on the basis of experimental measurements carried out on reference samples. The study on pure materials permitted the definition of marker bands, mainly combination and overtone modes, enhanced by the diffuse reflection component of the light, functional for the non-invasive pigment identification in real artworks. Several case studies are reported, including wall, easel, canvas paintings and manuscripts from ancient to modern art demonstrating the strengths of the technique on the identification of pigments even in the presence of complex mixtures of both organic (binders, varnishes) and inorganic (supports, fillers and other pigments) compounds.

1 Introduction

Fourier transform infrared spectroscopy (FT-IR) is a powerful technique for functional group analysis and molecular speciation of organic and inorganic chemical compounds. Thus, in research pertaining to Cultural Heritage, many studies regarding the characterisation of functional groups of pigments, fillers, binders and varnishes in paintings have been performed using either transmission or attenuated total reflection (ATR) infrared spectroscopy on micro-samples taken from the artwork [1–3 and references therein].

The availability of mid-IR fibre optics coupled with Fourier transform infrared benches has made possible to perform non-invasive reflection measurements from unique objects such as works of art, without any sampling or contact with the surface. Moreover, when the benches consist of portable FTIR spectrophotometers, non-invasive on site analyses on objects, which cannot or must not be moved from their current locations, are also possible.

Benefits and limitations of a non-invasive and in situ approach exploiting several integrated spectroscopic methods have been recently discussed [4] on the basis of the experience made within the activity of the European mobile laboratory MOLAB [5, 6].

Infrared reflection spectroscopy is a non-invasive and portable tool allowing one to gain valuable molecular information on a wide range of painting materials whilst fully respecting artwork integrity. However, despite the fact that it has been introduced in the conservation science field more than 10 years ago [7–11], reflection infrared spectroscopy has not yet become a routine method for analysing artwork materials. The main shortcoming regards the fact that reflection mode spectra can present odd distortions of band shape, position and intensity, which depend on several factors, such as absorption and refraction index and surface roughness, as discussed in the next paragraph. In consequence, the interpretation of reflection spectra of unknown heterogeneous materials more often than not turns out to be very challenging. Nevertheless, through systematic laboratory studies of the infrared reflection behaviour of reference Cultural Her-

C. Miliani (✉) · F. Rosi · B.G. Brunetti
Istituto CNR di Scienze e Tecnologie Molecolari (CNR-ISTM), c/o Dipartimento di Chimica, Università degli Studi di Perugia, via Elce di Sotto 8, 06123 Perugia, Italy
e-mail: miliani@thch.unipg.it

C. Miliani · F. Rosi · A. Daveri · B.G. Brunetti
Centro SMAArt, c/o Dipartimento di Chimica, Università degli Studi di Perugia, via Elce di Sotto 8, 06123 Perugia, Italy

itage materials (i.e., natural [12] and synthetic [13] organic binders, finishing materials [14], marble contaminants [15], preparation layers [16]) made possible to clear the path toward a conscious and at the same time fruitful interpretation of reflection spectra from real artworks.

The paper here presented intends to discuss the issues related to the reflection IR analysis of artists' pigments. A deep insight into their infrared spectral behaviour in the entire medium and a portion of the near infrared range (7000–900 cm^{-1}) is given, beyond what is already known from the otherwise abundant literature on the subject of transmission infrared spectroscopy of painting materials. Several series of in situ measurements carried out on ancient and modern paintings, realised with different techniques, are discussed, with the aim to show how reflection infrared spectroscopy can give valuable information on the molecular structure of a number of inorganic pigments, strongly reducing the necessity of carrying out micro-destructive analysis.

1.1 Principles of infrared reflection spectroscopy

When light strikes on the surface of a bulk material, it can be directly reflected without entering the sample or it can penetrate inside the bulk material, then be absorbed, refracted, reflected and scattered prior reaching again the surface and coming out as reflection beam. These two types of reflection are known as surface reflection (R_s) and volume reflection (R_v), respectively.

The surface reflection (also called specular reflection) is ruled by Fresnel's law (1) that explicates its dependency on both the absorption index (k) and refractive index (n) as follows:

$$R_s = \frac{(n-1)^2 + k^2}{(n+1)^2 + k^2} \tag{1}$$

In the case of surface reflection two types of spectral distortion are observable:

(i) derivative-like features characterise the spectra from samples with $k < 1$ (most organic molecules including polymers) following the profile of the refractive index n across the wavelength [17];
(ii) inverted or *reststrahlen* bands appear with strong oscillators that is for $k \gg 1$ (most inorganic salts containing oxyanions nitrates, carbonates, sulphates, phosphates) [17].

The volume reflection (also called diffuse reflection), being basically originated from an absorption process, gives rise to spectra very similar to those collected in transmission mode. Some differences in terms of relative band intensities, are generally observed since the penetration depth of diffuse reflected light is inversely proportional to both the scattering factor and the absorption coefficient [18]. Considering the variation of the scattering coefficient along the infrared range (3–11 μm) and assuming valid the condition for Rayleigh scattering (i.e. scattering coefficient is dependent on λ^{-4}, when the scattering centre is much smaller than the infrared wavelength [19]), the low wavenumber bands having a lower scattering coefficient are intensified with respect to the high wavenumber side region [20]. Moreover, the IR reflection measurements makes the effective sample thickness larger for weak absorption bands, which exhibiting a small absorption coefficient can travel long distance by repeated refractions. As a consequence, in volume reflection an enhancement of weak band intensity with respect to strong band intensity is generally observed.

Generally, the optical geometry of the fibre-optic portable infrared systems tends to maximise the specularly reflected light working with an angle of incidence equal to the reflected one (0°/0° in the present work). Nevertheless, in reflection infrared measurements of artworks, the surface reflection and volume reflection are generally both active, affecting the spectral features with a weight that depends not only on the materials optical properties but also on the roughness of the surface. As regard the morphological properties, optical flat surfaces (i.e. the dimensions of the particles are larger with respect to the infrared radiation wavelength) will provide a greater amount of the specular light; on the other side rougher surfaces (i.e. the particles have dimensions similar to the infrared radiation wavelength) will generate mainly diffuse reflected radiation. The optical properties both in terms of the absorption and refractive indices will influence the degree of penetration of the light and thus the contribution of the surface and volume reflection. Therefore, several types of distortion, due to derivative shape, reststrahlen effect, and intensity enhancement, can coexist in the same spectrum, making impossible the application of Kramers–Kronig and Kubelka–Munk corrections [17] thus rendering its interpretation not straightforward.

2 Experimental

Reference materials Commercially available materials have been selected on the basis of their chemical and mineralogical properties, according to their use in mural and easel paintings. The pigments under study have been purchased from Zecchi (azurite, malachite, lead white, red and yellow ochre, smalt, Sangiovanni white), Maimeri (ultramarine blue, lapis lazuli), Aldrich (cerussite, hydrocerussite, lead sulphate, barium sulphate, gypsum), or synthesised in the laboratory (anhydrite and bassanite); mineral celadonite and glauconite have been kindly provided by the Institute of Inorganic Chemistry of the ASCR (Czech Republic) whilst Egyptian blue by the British Museum, London. All the pigments have been previously characterised by transmission FTIR and X-ray fluorescence. Reflection infrared spectra

have been recorded on the pure pigment powder compressed in pellet.

Infrared reflection spectroscopy Reflection FTIR spectra were recorded using a portable JASCO VIR 9500 spectrophotometer equipped with a Remspec mid-infrared fibre optic sampling probe. The bench is made up of a Midac Illuminator IR radiation source, a Michelson interferometer and a liquid nitrogen cooled MCT (Mercury Cadmium Telluride). Notably it weighs only 35 kg and has overall dimensions of $50 \times 50 \times 50$ cm^3. Hence, it is portable and can be moved into museum rooms as well as onto scaffoldings at painting restoration worksites.

The fibre optic probe is a bifurcated cable containing 19 chalcogenide glass fibres, seven of which carry the infrared radiation from the source to the sample, whilst the other 12 collect the radiation reflected off the surface. The optical alignment of the Y probe end with source and detector focal points is guaranteed by a compact optical bench.

The chalcogenide glass fibres allow for the collection of spectra from 6000 to 900 cm^{-1}, having an excellent signal-to-noise ratio throughout the range except in the 2200–2050 cm^{-1} region due to the Se–H stretching absorption. In the present study, 400–800 interferograms were collected covering a spectral range from 6000 to 900 cm^{-1} at a resolution of 4 cm^{-1}.

The fibre optic probe is kept strictly perpendicular to the sample surface (normal geometry) by a mechanical arm. The distance between the probe and the surface is fixed at about 5 mm by a distance device, in order to avoid the contact between fibres and sample. The width of the investigated sample area is determined by the probe diameter which is about 4 millimetres.

The total reflectance R (from the combined diffuse and specular components) is measured using the spectrum from an aluminium mirror plate as background. The spectrum intensity unit was defined as the absorbance A' obtained from R by $A' = \log(1/R)$.

3 Results and discussion

The spectroscopic library here presented is intended to allow a rapid identification of a pigment through non-invasive reflection IR spectroscopy. The spectra of the standard pigments are discussed by the functional group which characterised their chemical formula, namely carbonates, sulphates and silicates. These functional groups have been selected because, differently from other class of pigment such as oxides and sulphides, exhibit absorptions in the region of interest for fibre optic reflection spectroscopy, i.e. 6000–900 cm^{-1}.

3.1 Carbonates

3.1.1 Azurite ($2CuCO_3Cu(OH)_2$), malachite ($CuCO_3Cu(OH)_2$), Sangiovanni white ($CaCO_3$), lead white (cerussite $PbCO_3$ and hydrocerussite $2PbCO_3Pb(OH)_2$)

Inorganic carbonates have been used as pigments since antiquity; they comprise many minerals such as calcite, dolomite, azurite and malachite and also some synthetic metallic salts such as lead white (a mixture of neutral and basic lead carbonate) and Sangiovanni white [21]. Transmission infrared spectra of carbonates show four prominent absorption bands of CO_3^{-2} moiety in the regions 1390–1500 (ν_3 antisymmetric stretching), 800–900 (ν_2 out-of-plane bending), 680–780 (ν_4 in-plane bending) and 1000–1100 cm^{-1} (ν_1 symmetric stretching) [22]. These bands, being unique in position and shape for each metallic carbonate, are diagnostic of molecular composition of the various pigments. Moreover, it has been recently proved on archaeological samples that infrared transmission features may enable one differentiating even between calcite minerals with different origin [23].

Additionally, basic carbonates show also the fundamental OH stretching modes at about 3425 cm^{-1} for azurite, at 3400–3320 cm^{-1} as doublet for malachite and at 3535 cm^{-1} for hydrocerussite [22].

In reflection mode through a fibre optic probe, the deformation modes ν_2 and ν_4 are not accessible lying below 900 cm^{-1}. As foreseen by Fresnel's law, the strong absorption in the region 1450–1420 cm^{-1} related to the antisymmetric CO_3^{-2} stretching (ν_3), is inverted by the *reststrahlen* effect, whilst the low absorption, due to symmetric CO_3^{-2} stretching (ν_1) around 1000 cm^{-1}, has a derivative shape (Fig. 1). Except the OH stretching mode of hydrocerussite at about 3540 cm^{-1}, the corresponding vibrational modes in azurite and malachite appear with a derivative shape in reflection mode. As a consequence, the first-order bands generally considered as diagnostic features for the interpretation of transmission mode spectra of carbonate pigments cannot be employed for the assignment of reflection spectra of unknown samples.

On the other hand, further features related to combination (sum or difference of fundamental bands) and overtones bands clearly emerge in reflection spectra. These bands, being forbidden, exhibit small absorption coefficients; therefore, whilst not subjected to specular distortions, they are effectively enhanced by volume reflection. The shape and position of combination and overtones bands of each carbonate pigments are visible in Fig. 2 and their tentative assignments are provided in Table 1.

The combination band at lower wavenumber is assigned to the $\nu_1 + \nu_4$ mode [24, 25] it appears: at about 1860 cm^{-1}

and broad for azurite, at 1733 and 1740 cm^{-1} and sharp for cerussite and hydrocerussite, at 1800 cm^{-1} and structured for malachite, at 1800 cm^{-1} and sharp for Sangiovanni's white (Fig. 2a). It is worth noting that the $\nu_1 + \nu_4$ combination mode can be mistaken with the carbonyl antisymmetric stretching band of a lipidic binder [12], thus special attention must be paid in the binder identification when lead white is present. The next combination band, occurring in the region 2800–2300 cm^{-1}, is most probably due to the $\nu_1 + \nu_3$ coupling [15, 26], although other authors assigned it to a $2\nu_2 + \nu_4$ mode [25].

This region shows bands that, for shape and position, are very specific for each carbonate structure, accounting for the specificity of the sym and antisymmetric stretching modes themselves (Fig. 2b). Azurite exhibits a $\nu_1 + \nu_3$ combination band with three resolved contributions at 2500, 2553, 2587 cm^{-1}, diversely malachite shows two bands at 2423 and 2542 cm^{-1}. Sangiovanni's white is characterised by a $\nu_1 + \nu_3$ combination band centred at 2512 cm^{-1} with a prominent shoulder at 2594 cm^{-1}, whilst as regards lead white, cerussite and hydrocerussite exhibit a broad band at 2410 and 2428 cm^{-1}, respectively. Additionally cerussite shows an unassigned feature positioned at 2040 cm^{-1} not observed in the hydrous form of the lead carbonate (Fig. 1b). In the same spectral range, also malachite has a characteristic weak band at 2077 cm^{-1} (Fig. 1c).

Another region of interest is that toward the near infrared as reported in Fig. 2c, where the overtone $3\nu_3$ [25] as well as the bands due to $\nu + \delta$ (OH) [27] occur, this last in the case of basic carbonates such as azurite, malachite and hydrocerussite. In particular, azurite exhibits as strong doublet at 4380 and 4244 cm^{-1} that can be ascribable to both combination $\nu + \delta$ (OH) and overtone $3\nu_3$. The doublet only partially overlays with the combination of methylenic C–H stretching and bending of lipidic binders [27], and azurite can also be identified when applied with a drying oil. The same mode appears with lower intensity at 4408 and 4242 cm^{-1} for malachite and at 4300 cm^{-1} for hydrocerussite. Most probably the signal at 4264 cm^{-1}, visible in the reflection spectrum of Sangiovanni white is due to the second harmonic of the antisymmetric stretching of carbonate.

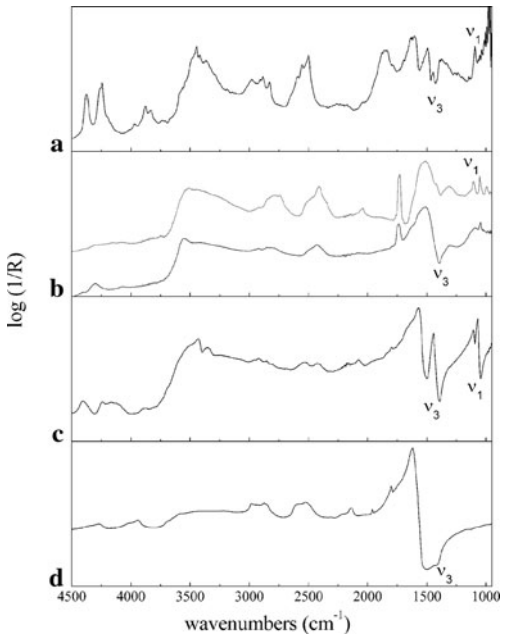

Fig. 1 Reflection mode spectra in the region 4500–950 cm^{-1} of carbonate pigments: (**a**) azurite ($2CuCO_3Cu(OH)_2$); (**b**) lead white, cerussite ($PbCO_3$, *light grey line*) and hydrocerussite ($2PbCO_3Pb(OH)_2$), *dark grey line*); (**c**) malachite ($CuCO_3Cu(OH)_2$); (**d**) Sangiovanni white ($CaCO_3$)

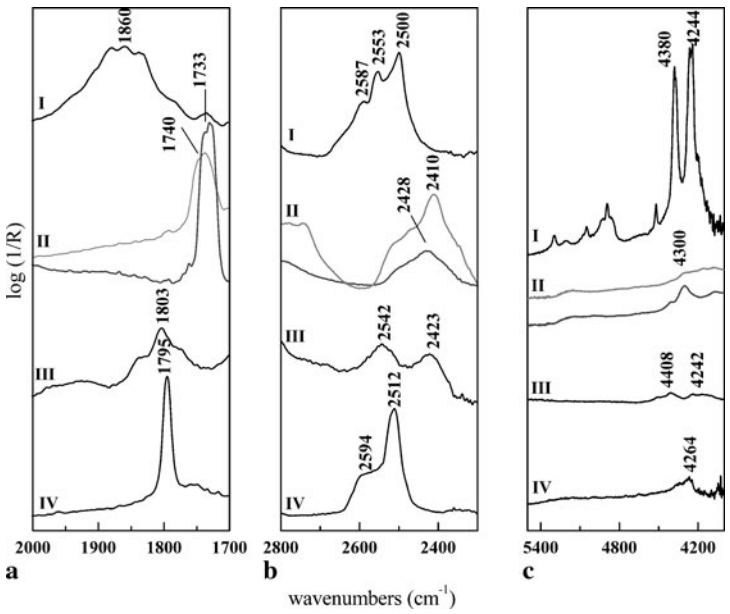

Fig. 2 Reflection mode spectra of carbonate pigments in the regions of combination and overtones bands: (**a**) combination $\nu_1 + \nu_4$; (**b**) combination $\nu_1 + \nu_3$; (**c**) overtone $3\nu_3$ and combination $\nu + \delta$ (OH). Labels I, II, III, IV indicate azurite, lead white (*dark grey line*—hydrocerussite, *light grey line*—cerussite), malachite and Sangiovanni white, respectively

Table 1 Experimental wavenumber values of combination and overtone modes in carbonates and their tentative assignment

Azurite	Malachite	Cerussite	Hydrocerussite	Sangiovanni white	Assignment
1860	1800	1733	1740	1800	$\nu_1 + \nu_4$ (CO_3^{-2})
2500, 2553, 2587	2423, 2542	2410	2428	2512, 2594sh	$\nu_1 + \nu_3$ and/or $2\nu_2 + \nu_4$ (CO_3^{-2})
4380, 4244	4408, 4242		4300	4264*	$3\nu_3$ (CO_3^{-2}) and $\nu + \delta$ (OH)

* for Sangiovanni white this band corresponds to $3\nu_3$ (CO_3^{-2})

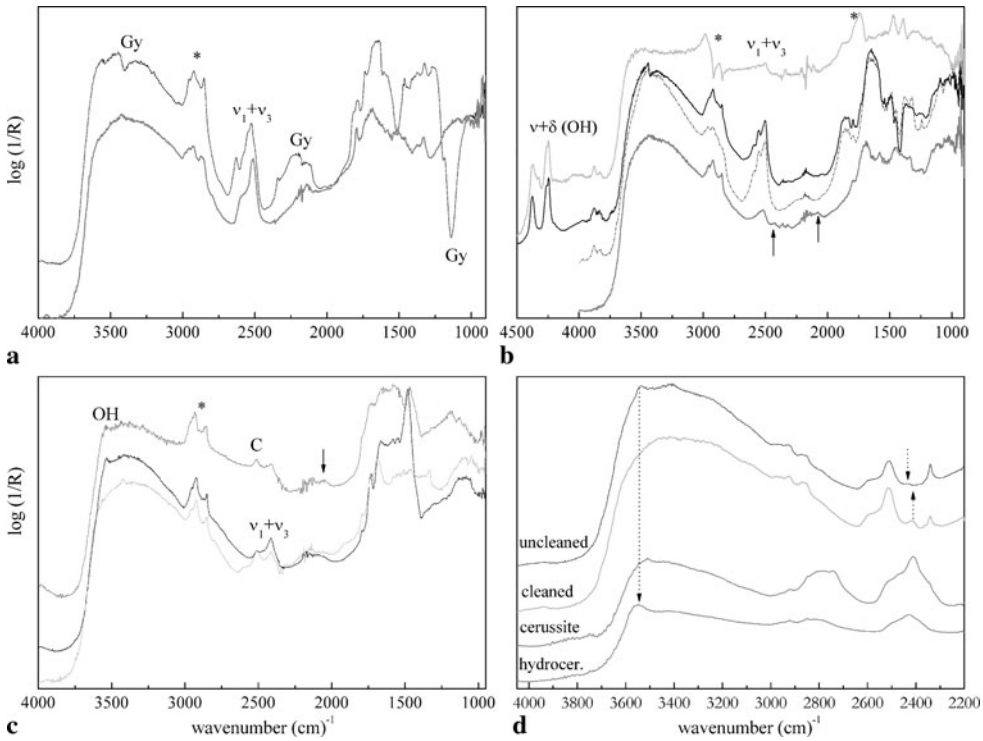

Fig. 3 Examples of non-invasive reflection spectra acquired on real artworks painted with carbonate pigments. (**a**) *calcite/dolomite*: white background from a Renaissance wall painting by B. Gozzoli in the San Girolamo chapel in Montefalco (1452 Perugia, Italy)—*grey line*—; white area of a Roman wall painting located in the Pompei archaeological site (*Casa del Bicentenario* Napoli, Italy)—*black line*—. (**b**) *azurite*: blue decoration on a Romanian illuminated medieval manuscripts (*Four Gospels Book of Humor*, Putna Monastery, Romania)—*black line*—; blue mantle (*dash dot black line*) with greenish shadow (*grey line*) from Renaissance mural painting by il Perugino (*Adorazione dei Magi*, Trevi, Italy); blue mantle form the painting *La Bella* by Tiziano (1536, Galleria degli Uffizi Firenze, Italy)—*light grey line*—. (**c**) *lead white*: white areas of the Romanian manuscript—*black line*— and Benozzo's wall painting—*light grey line*—; white area of Cezanne's painting *La route tournante* (1902, Courtauld Institute of Art Gallery London UK)—*grey line*—. (**d**) *lead white*: white area of A. Gaddi's mural painting (*Le Storie della Vera Croce*, 1380–1390, the Cappella Maggiore in S. Croce, Firenze, Italy), before (*black line*) and after (*light grey line*) a cleaning test with NH_4HCO_3. For all the graphs, asterisks indicate signals of organic binders, C and Gy stand for calcite and gypsum, respectively

3.1.2 Identification of carbonate pigments on real artworks

All these secondary features, usually not considered in transmission mode where the fundamental bands are prominent, become diagnostic bands in reflection mode spectra allowing for the non-invasive identification of carbonate pigments in different types of objects and matrices, such as oil [28] and tempera [29] ancient easel paintings, modern paintings [30], painted ceramics [31], wall paintings [32] and manuscripts [33].

In Fig. 3, some examples of reflection mode spectra acquired in situ on different types of polychrome objects painted with carbonate pigments are shown (in all the graphs asterisks indicate signals coming from the different organic binders).

Exploiting the specificity of the undistorted $\nu_1 + \nu_3$ combination band of the carbonate anion it has been possible to identify and distinguish the Sangiovanni white, mainly composed of calcite, from dolomite, the magnesium and calcium carbonate $Ca,Mg(CO_3)_2$ often found in Roman wall paint-

ings [34]. In Fig. 3a, the spectrum collected from the white background of a Renaissance wall painting by Benozzo Gozzoli is compared with the spectrum acquired on a white area of a Roman wall painting. The spectrum from the Renaissance painting clearly shows the typical combination band $\nu_1 + \nu_3$ at 2512 cm^{-1} of calcite indicating the use of Sangiovanni white. Conversely the Roman wall painting show in the same region a well structured band with at least three maxima at 2524, 2547 and 2629 cm^{-1} assigned to the combination $\nu_1 + \nu_3$ (CO_3^{-2}) of dolomite [35]. This spectrum also contains the vibrational signatures of gypsum that will be discussed in the next paragraph.

Analogously, the non-invasive identification of azurite on real artworks is generally easily accomplished by observing the typical $\nu_1 + \nu_3$ combination of the copper carbonate. In Fig. 3b, this band is clearly observed in the spectra collected from a Romanian illuminated medieval manuscripts—black line and from a Renaissance mural painting by il Perugino [32]. Furthermore, the presence of the $\nu_1 + \nu_3$ band at about 2420 cm^{-1} along with the weak peak at 2080 cm^{-1} allowed also for the identification of malachite in mixture with azurite in Perugino's painting (Fig. 3b) [32]. In the case of the blues of the manuscript and of the mural (Fig. 3b), the typical spectral profile of azurite in the range 2000–1400 cm^{-1}, containing the fundamental ν_3 and the $\nu_1 + \nu_4$ combination, is also observable thanks to the low spectral interference of the corresponding substrata ($CaCO_3$-mortar, parchment and binders) probably related to a relatively high concentration of the pigment.

When the surface of the investigated artwork is smooth enough to generate a stronger contribution of surface reflection, as it could be for easel or panel paintings usually painted with a finishing layer of shiny and optically flat varnish, the combination bands in the range 1800–2800 cm^{-1} may not be visible. As an example, the spectrum collected on the panel painting *La Bella* by Tiziano (1536, Galleria degli Uffizi Firenze, Italy) [36] is reported in Fig. 3b showing a too weak $\nu_1 + \nu_3$ combination band for a certain identification of azurite. Nevertheless, the high wavenumber region (above 4000 cm^{-1}) being characterised by bands with less intense absorption coefficients allows for a deeper penetration depth and a bigger contribution of the volume reflection. As a result, the $\nu + \delta$(OH) of azurite are clearly evident to ensure the presence of the blue copper carbonate pigment in the painting.

The non-invasive identification of lead white (Fig. 3c) is often accomplished still locating the $\nu_1 + \nu_3$ combination band of the carbonate anion shifted to lower wavenumbers (at about 2400–2420 cm^{-1}) with respect to the other white carbonate pigments (calcite and dolomite). In Fig. 3c some examples of spectra collected from white areas of the already mentioned Romanian manuscript, Benozzo's wall painting, and Cezanne's painting *La route tournante* (1902, Courtauld Institute of Art Gallery London UK) [37] are reported. Whilst the 2400 cm^{-1} band can be used for discriminating white lead from the other carbonate pigments (in the present case calcite labelled C has been detected Fig. 3c), the distinction of cerussite and hydrocerussite is rarely possible on real artworks by taking into account the difference of about 18 cm^{-1} of the broad $\nu_1 + \nu_3$ (CO_3^{-2}) bands corresponding to the anhydrous and hydrous forms of lead white. More precisely, in the reported spectra of Fig. 3c, the discussed band is positioned at 2410 cm^{-1} suggesting the presence of cerussite, the broadness of this feature avoids the visualisation of the possible contribution at 2428 of hydrocerussite which, nevertheless, can be identified by the specific O–H stretching at 3540 cm^{-1} (as in the cases of the Romanian manuscript and Cezanne painting, Fig. 3c).

In the last graph (d) of Fig. 3 the spectra collected from a white area of a mural painting by Agnolo Gaddi are reported and compared with the reflection spectra of cerussite and hydrocerussite reference. The two spectra, collected from the mural, have been acquired on the same point before and after a cleaning test with NH_4HCO_3. The spectrum from the unclean area is composed mainly of hydrocerussite clearly detected by the OH stretching band at about 3540 cm^{-1} and by the weak feature at 2430 cm^{-1} ($\nu_1 + \nu_3$ (CO_3^{-2})). After the treatment with NH_4HCO_3 both of these bands disappear and simultaneously a new feature at 2410 cm^{-1} assigned to $PbCO_3$ becomes evident suggesting that the cleaning method may cause the conversion of hydrocerussite into cerussite, without, however, affecting the colour or the general appearance of the painted surface.

3.2 Sulphates

3.2.1 Barite ($BaSO_4$), anglesite ($PbSO_4$), gypsum ($CaSO_4 2H_2O$), bassanite ($CaSO_4 0.5H_2O$), anhydrite ($CaSO_4$)

Sulphate compounds are of great interest as Cultural Heritage materials being widely used as white pigments or fillers in paint and preparation layers of ancient as well as modern easel paintings. The tetrahedral anion SO_4^{2-} exhibits nine normal modes [22]: a symmetric stretch, ν_1 (1000 cm^{-1}), a doubly degenerate symmetric bending, ν_2 (400–500 cm^{-1}), a triply degenerate asymmetric stretching ν_3 (1050–1250 cm^{-1}) and a triply degenerate bending ν_4 (500–700 cm^{-1}). Metal complexation and variation in coordination of water molecules can modify the S–O bond lengths, hence in sulphate minerals the symmetry of the anion are lowered. As a result, IR-forbidden vibrations are permitted, degenerate vibrations are split, and fundamental vibrations are shifted.

In Fig. 4 the reflection spectra of three different white sulphates, anglesite ($PbSO_4$), barite ($BaSO_4$) and gypsum ($CaSO_4 2H_2O$), are shown. Although the lowering of the

symmetry made the degeneracy of asymmetric stretching ν_3 to be removed, the resulting splitting in two resolved bands for anglesite (1163, 1047 cm^{-1}) and gypsum (1146, 1118 cm^{-1}) and in three bands for barite (1205, 1136, 1100 cm^{-1}) are no longer observed in reflection mode. In fact, due to their high absorption index k, all the ν_3 bands are affected by the *reststrahlen* effect and consequently appear as inverted bands showing their minima at about 1059 cm^{-1}, 1067 cm^{-1} (structured band), 1160 cm^{-1}, for anglesite, barite and gypsum, respectively. The enhancement of second-order and combination bands, due to diffuse reflection, is evident in the range 2500–1900 cm^{-1} for all the three sulphates. The $2\nu_1$ mode is positioned at 1933, 1965 and 2010 cm^{-1} for anglesite, barite and gypsum respectively. The combination $\nu_1 + \nu_3$ gives rise to a system of bands which are positioned at 2010 and 2115 cm^{-1} for anglesite, at 2064, 2132 and 2190 cm^{-1} for barite. At higher wavenumbers, the $2\nu_3$ band is placed at 2327 and 2335 cm^{-1} for lead and barium sulphate respectively. In the reflection spectrum of gypsum both the modes $\nu_1 + \nu_3$ and $2\nu_3$ are covered by a strong and broad band at 2230 cm^{-1} probably due to the combination of bending and libration modes of H_2O ($\nu_2 + \nu_L$) [16]. The experimental wavenumbers of harmonic and combination bands of sulphates and their assignment are summarised in Table 2.

Therefore through reflection IR spectroscopy a non-invasive speciation of sulphate white pigments with respect to the coordination metal (lead, barium or calcium) can be carried out evaluating the shape and position of ν_3 *reststrahlen* band or the combination and overtone bands in the range 2500–1900 cm^{-1}.

Recently Rosi et al. [16] have investigated the reflection IR properties of the $CaSO_4$–H_2O system (gypsum/bassanite/anhydrite) evaluating the spectral distortion of fundamental bands and assigning the SO_4^{2-} overtone and combination bands in the range 2500–1900 cm^{-1}. In this case the inverted ν_3 *reststrahlen* band cannot be used for the identification of hydration state, since the small differences in shape and position of the antisymmetric stretchings are not appreciable when the reflection distortion occurs. Conversely, as is possible to observe in Fig. 5, the combination and overtone bands are different enough to be used as diagnostic features to non-invasively discriminate between gypsum, bassanite and anhydrite (see Table 2, for the assignment).

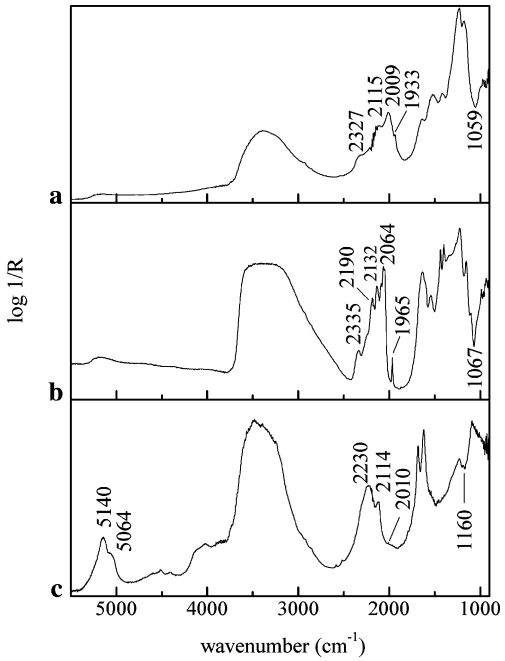

Fig. 4 Reflection spectra in the region 950–5500 cm^{-1} of white sulphate pigments: (**a**) anglesite ($PbSO_4$), (**b**) barite ($BaSO_4$), (**c**) gypsum ($CaSO_4 2H_2O$)

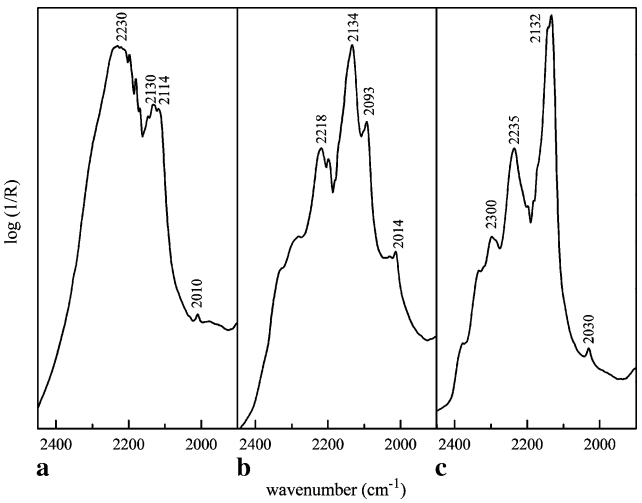

Fig. 5 Reflection spectra of (**a**) gypsum ($CaSO_4 2H_2O$), (**b**) bassanite ($CaSO_4 0.5H_2O$) (**c**) β-anhydrite ($CaSO_4$) in the range of second-order and combination modes (modified from [16])

Table 2 Experimental wavenumber values of combination and overtone modes in sulphates and their tentative assignment

Anglesite	Barite	Gypsum	Bassanite	Anhydrite	Assignment
1933	1965	2010	2014	2030	$2\nu_1$ SO_4
2009, 2115	2064, 2132, 2190	2114, 2132	2093, 2134	2132, 2141	$\nu_1 + \nu_3$ SO_4
2327	2335	2230	2218	2235	$2\nu_3$ SO_4; $\nu_2 + \nu_L$ H_2O*
–	–	5064, 5140	5212	–	ν_1/ν_3 OH + ν_2 OH

* only for gypsum

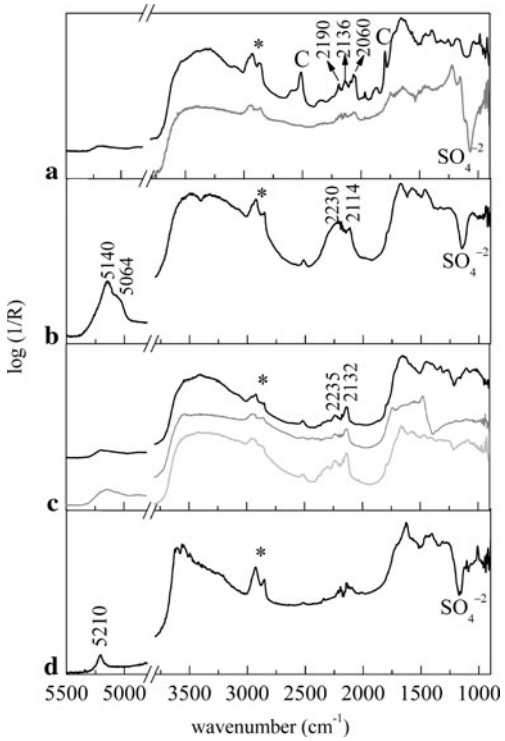

Fig. 6 Examples of non-invasive reflection spectra acquired on real artworks painted with white sulphate pigments. (**a**) *barite*: white area of the oil painting *Victory Boogie Woogie* by Modriaan (1942–1944, Gemeentemuseum, Den Haag, Netherlands)—*black line*—, white area of the painting *Bianco 1952* by Burri (Collezione Albizzini, Città di Castello, Italy)—*grey line*—; (**b**) *gypsum*: lacuna on the painting *Deposizione Baglioni* by Raphael (1507, Galleria Borghese Roma, Italy); (**c**) *anhydrite*: lacuna on the painting *Madonna del Cardellino* by Raphael (1506, Musei degli Uffizi Firenze, Italy)—*grey line*—, lacunas of *La Deposizione* by Bronzino (1545, Musée des Beaux-Arts, Besancon, France)—*light grey line*—, and *L'Assunzione e Incoronazione della Vergine* by Vasari (1567, S. Flora and Lucilla's Badia Arezzo, Italy)—*black line*—; (**d**) *bassanite*: 17th century reverse glass painting

3.2.2 *Identification of sulphate white pigments on real artworks*

The discussion on the non-invasive identification of white sulphate-based pigments is carried out presenting the spectra collected from different artworks (including modern and ancient paintings as well a 17th century reverse glass painting), showed in Fig. 6. Barium sulphate, used both as white pigment as well as extender and filler of commercial modern pigment formulations, can be easily identified either by using the typical ν_3 (SO_4^{-2}) *reststrahlen* band at about 1070 cm^{-1} or exploiting the $\nu_1 + \nu_3$ (SO_4^{-2}) combination bands in the 2500–1900 cm^{-1} range. The spectrum of Fig. 6a (grey line) has been acquired from a white area of the oil painting *Victory Boogie Woogie* by Mondriaan [38]. The smooth surface of the painting favours the collection of the surface reflected light generating an evident inverted band assigned to the asymmetric stretching of the sulphate anion in $BaSO_4$. Conversely, in the painting *Bianco 1952* by Burri [39], organic and inorganic fillers provide a rough surface favouring the diffuse reflected light and enhancing the typical combination band of $BaSO_4$ in the 2500–1900 cm^{-1} region.

Figure 6b–d contains the spectra collected in different artworks highlighting the possibility of non-invasively identify the different hydration phases of Ca–sulphates pigment [16]. Precisely, in Fig. 6b the spectrum of a typical gypsum-glue-based preparation is reported. It has been collected from a lacuna on the painting *Deposizione Baglioni* by Raphael [16, 29]. A strong inverted band at 1150 cm^{-1} indicates the presence of a Ca-sulphate compound, nevertheless only the observation of the spectral features in the range 2500–1900 cm^{-1} and the well defined shape of the $\nu + \delta$ (OH) at 5140 cm^{-1} of hydration water coordinated in gypsum permitted the identification of the di-hydrate form of $CaSO_4$. Interestingly, the infrared reflection study of a coeval painting still by Raphael (*Madonna del Cardellino* [40]) revealed the presence in the preparation layer of the insoluble anhydrite (Fig. 6c grey line) in spite of gypsum. In the same figure, further spectra collected on Renaissance paintings namely *La Deposizione* by Bronzino and *L'Assunzione e Incoronazione della Vergine* by Vasari [41] show the typical combination band in the range 2500–1900 cm^{-1} of anhydrite. Finally, in a 17th century reverse glass painting the hemihydrate form-bassanite has been revealed (Fig. 6d), although the weakness of the combination band in the 2500–1900 cm^{-1} range, probably due to the presence of an optically flat surface, the typical $\nu + \delta$ (OH) sharp peak at about 5200 cm^{-1} of the hemihydrate calcium sulphate allowed for the identification of bassanite [16, 42].

3.3 Silicates

3.3.1 *Ultramarine blue* ($[Al_6Si_6O_{24}]S_n$), *smalt* ($CoO{\cdot}nSiO_2$), *green earth* ($[(Al^{III}, Fe^{III})(Fe^{II}, Mg^{II})]$, *kaolin* ($AlSi_3, Si_4)O_{10}(OH)_2$), *red ochre* ($Fe_2O_3$ + *clay* + *silica*), *yellow ochre* ($Fe_2O_3H_2O$ + *clay* + *silica*) *and Egyptian blue* ($CaCuSi_4O_{10}$)

Silicate pigments comprise a large number of natural and synthetic compounds all characterised by the presence of SiO_4 tetrahedral units, but showing very different structures, varying from the glassy phase of smalt [43] to the ordered sodalite network of lapis lazuli [44]. Whatever is the crystalline structure, all silicates absorb strongly in the range 1100–800 cm^{-1} with intense Si–O antisymmetric stretching modes. Although the environment of the silicate ion varies from one mineral group to another affecting the shape and frequency of the absorption band, a certain identification of the silica-based pigment only on the basis of infrared is very often not feasible since in reflection mode the strong sili-

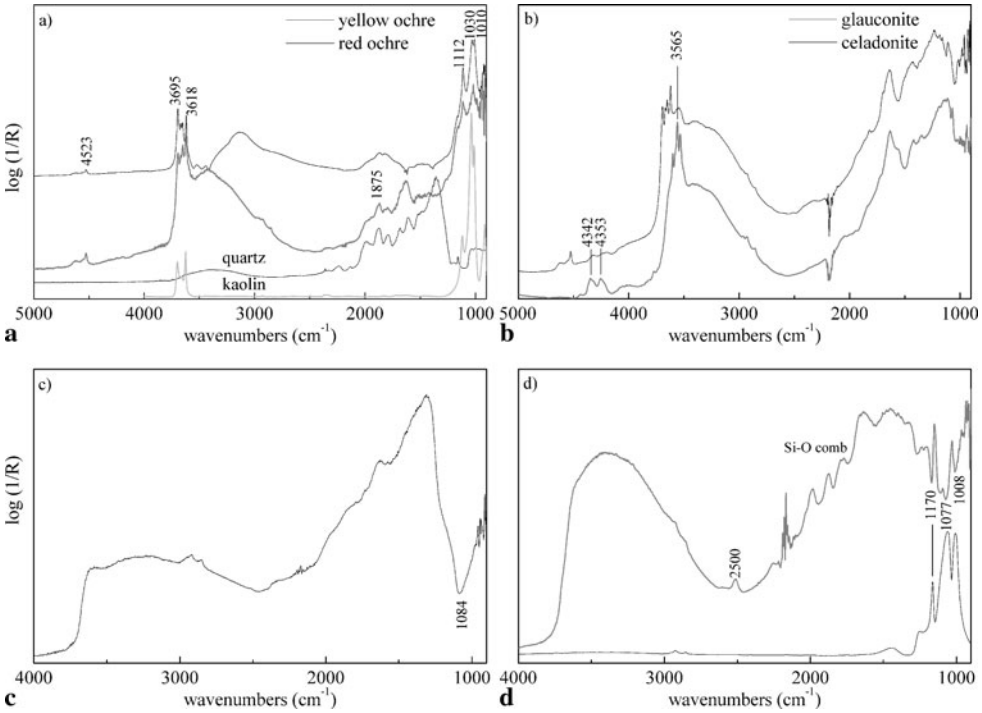

Fig. 7 Reflection mode spectra of silicate pigments: (**a**) red and yellow ochre compared with the spectra of kaolin in transmission mode and of quartz in reflection mode; (**b**) green earth (glauconite and celadonite); (**c**) smalt; (**d**) Egyptian blue

cate mode is distorted by the surface reflection generating *reststrahlen* bands.

In the case of red and yellow iron earth pigments, the colour is produced by Fe (III) oxides and hydroxides whose infrared bands fall out of the achievable range by the fibre optic portable equipment [45]. Generally, the infrared study provides for the identification of the accessory minerals such as quartz, clays, carbonates, sulphates. In Fig. 7a the reflection spectra of red and yellow ochre are reported along with a transmission spectrum of kaolin (from IRUG database [46]) and a reflection spectrum of quartz. In both pigments kaolin is clearly evident by the fundamental Si–O stretching mode at 1100–1010 cm^{-1} and OH stretching at 3600 cm^{-1} and the combination band $\nu + \delta$ (OH) at 4523 cm^{-1} [47, 48]. In red ochre pigment also the presence of quartz is underlined by the combination bands $\nu + \delta$ (Si–O) in the range 2000–1700 cm^{-1} [35].

Green earths are mainly composed of clay micas celadonite $(K[(Al,Fe^{3+}),(Fe^{2+},Mg)]\ (AlSi_3,Si_4)O_{10}(OH)_2)$ and glauconite $(K,Na)\ (Fe^{3+},Al,Mg)_2,(SiAl)_4O_{10}(OH)_2)$. In spite of having a similar molecular composition they have different mineral origins, thus the possibility to distinguish them in artistic painting could provide useful information on the pigment provenance [49]. Concerning IR reflection spectroscopy, both minerals have strong absorption bands of Si–O stretching at about 1100–900 cm^{-1} often resulting as distorted inverted peaks not useful for their identification (Fig. 7). Differently, the sharp and distinct peaks in the OH stretching region (3600–3530 cm^{-1}) in celadonite [50] along with characteristic doublet $\nu + \delta$ (OH) at 4340 and 4353 cm^{-1} can be used for its identification and distinction from glauconite. The latter is in fact characterised by a more disordered structure of the cation in the octahedral sheet giving weaker and broader infrared spectral features [51]. Glauconite is also less pure and it can be found in mixture with other clay minerals as montmorillonites, chlorites and kaolin according to the source locality. The investigated glauconite reference sample contains also kaolin (Fig. 7), generally present as secondary mineral in glauconitic clays of Cretaceous age in the Prague area (which is the provenance of the investigated celadonite and glauconite reference samples) [52].

Smalt is a blue Co-coloured potassium glass used as pigment since ancient times [43]. The infrared reflection spectrum of a reference pigment is reported in Fig. 7c showing a strong and most probably inverted band assigned to Si–O asymmetric stretching at about 1080 cm^{-1} related to the glassy matrix. The silicate network does not provide further marker bands of the pigment thus making the identification possible only combining the infrared study with other spectroscopic techniques, i.e. the elemental XRF analysis able to detect the presence of cobalt. Conversely, it has been already demonstrated the possibility of investigating the electronic properties of smalt pigment in the near infrared region in order to distinguish among the different Co-based blue pigments [28, 37, 53].

Egyptian blue is the first synthesised pigment extensively used from the early dynasties in Egypt and during the Roman period in Europe. The infrared spectrum of the copper calcium silicate pigment, whose mineral counterpart is

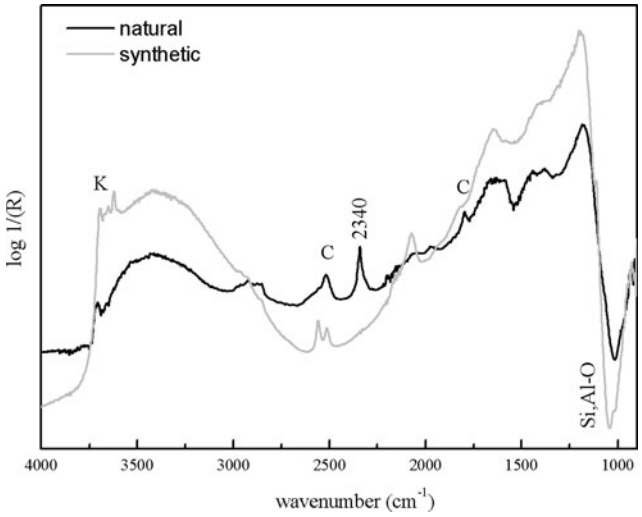

Fig. 8 Comparison between reflection mode spectra of natural (*black line*) and synthetic (*grey line*) ultramarine blue pigments. K and C stand for kaolin and calcite, respectively

cuprorivaite, shows distinct bands in the Si–O region (1100–1000 cm^{-1}) that can be used for its identification also in reflection mode. The characteristic peaks assigned to cuprorivaite at 1160, 1060 and 1008 cm^{-1} (Fig. 7d, black line) [54] are present in the reflection spectrum mainly as inverted bands positioned at 1170, 1077 and 1008 cm^{-1} (Fig. 7d, grey line); the region 2000–1800 cm^{-1} is characterised by the combination bands ($\nu + \delta$) Si–O [35].

The case of natural and synthetic ultramarine pigments deserves a special mention. They are both feldspathoids with the ideal formula $Na_{7.5}[Al_6Si_6O_{24}]S_{4.5}$ [55], where di- and tri-sulphur radical anions are the chromophores (yellow S_2^- and blue S_3^-). The framework of alluminosilicate-sodalite $[Al_6Si_6O_{24}]^{6-}$ consists of alternating AlO_4 and SiO_4 tetrahedra which are linked to give cubo-octahedral cavities (sodalite β-cage) which host the chromophores. Natural ultramarine blue, extracted from the lapis lazuli stone, found in Europe its most extensive use in the fourteenth and mid-fifteenth centuries, whilst the synthetic route to produce artificial ultramarine blue was discovered by J.B. Guinet in 1830. Despite the fact that the two pigments share the same molecular structure, they can be differentiated non-invasively employing reflection infrared spectroscopy thanks to the presence in the spectrum of the natural pigment of a distinctive signal from a very specific impurity: the stretching of carbon dioxide entrapped in the sodalite cages [44].

In Fig. 8 the reflection infrared spectra of natural and synthetic ultramarine pigments are shown. The spectra are both characterised by fundamental vibrations of the framework Al,Si–O_4 whose strongest vibration appearing as *reststrahlen* band at 1010 cm^{-1} is assigned to an Si,Al–O asymmetric stretching of internal tetrahedra. The main differences between the spectra of natural and synthetic ultramarine are related to the presence of reagent residues such as kaolin in the synthetic pigment (OH stretchings at 3624 and 3700 cm^{-1}) and calcite, an associated mineral, in the natural pigment (combination bands at 2512 and 1800 cm^{-1}). In addition, a specific feature is visible at 2340 cm^{-1} as a strong and sharp band, only in the natural pigment. It has been assigned by Miliani et al. [44] to the antisymmetric stretching of carbon dioxide molecules which are retained in the structure from the lapis lazuli rock genesis, being encapsulated in the sodalite cages. Hence, the carbon dioxide absorption can be used as a diagnostic feature for distinguishing between natural and synthetic ultramarine pigments by non-invasive reflection infrared spectroscopy [4, 44].

3.3.2 *Identification of silica-based pigment on real artworks*

Figure 9 reports some infrared reflection spectra collected by the portable fibre optic system from real artworks. The spectrum in Fig. 9a has been collected from the Renaissance fresco by il Perugino previously mentioned, specifically on the blue Virgin's dress [32]. Besides the infrared spectral features of the carbonate plaster (C, at about 2500 cm^{-1} $\nu_1 + \nu_3$ of CO_3^{-2}) and the proteinaceous binder (B, CH stretching at about 2900 cm^{-1} and amide I and II in the range 1680–1540 cm^{-1}) an inverted band positioned at about 1070 cm^{-1} indicates the presence of a silicate component suggesting the possible presence of smalt as blue pigment. The certain identification of the pigment has been achieved only by combining the vibrational information with elemental XRF investigation which effectively revealed the presence of Co and the typical impurities of the pigment namely As, Bi and Ni [32].

A green earth-based pigment, mainly composed of celadonite, has been identified on a green background of the wall painting by Agnolo Gaddi in Florence. The spectrum reported in Fig. 9b (black line) is compared with the reference standard of celadonite (grey line) underlying the correspondence in the unknown spectrum of the fundamental ν (OH) and $\nu + \delta$ (OH) bands of the green clay pigment. Also in this case, the presence of infrared signals coming from the carbonate substrate (C) and other components of the painting (binder—B, oxalates—Ox) does not interfere with the identification of the green pigment.

In Fig. 9c the spectrum collected from a blue fragment coming from Roman mural painting debris (I–II century A.C.) found in the archaeological site *Urvinum Hortense Domus* of Collemancio (Perugia, Italy) is compared with that Egyptian blue reference. Except the stronger signals coming from the $CaCO_3$ substrate in the unknown sample, the structured reflection infrared features of cuprorivaite are clearly evident indicating the presence of Egyptian blue in

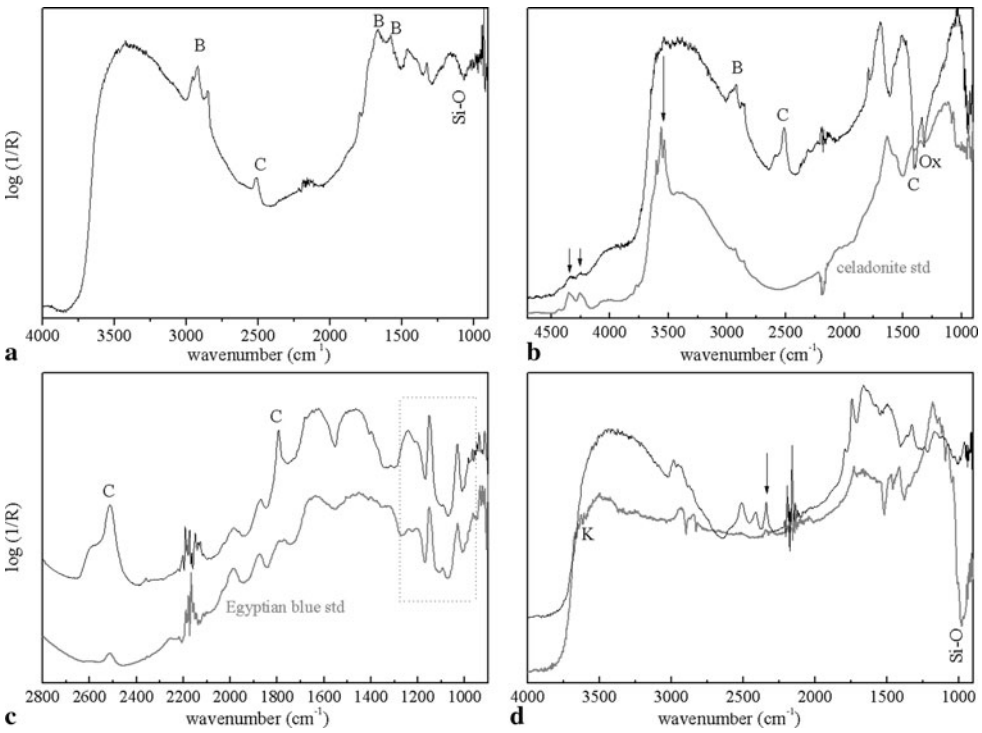

Fig. 9 Examples of non-invasive reflection spectra acquired on real artworks painted with silicate pigments. (**a**) *smalt*: Virgin's dress on the Renaissance mural painting by il Perugino (*Adorazione dei Magi*, Trevi, Italy). (**b**) *green earth*: green background on A. Gaddi's mural painting (*Le Storie della Vera Croce*, 1380–1390, the Cappella Maggiore in S. Croce, Firenze, Italy). (**c**) *Egyptian blue*: blue wall painting fragment the *Urvinum Hortense Domus* of Collemancio (Perugia, Italy). (**e**) *ultramarine blue*: *synthetic*, blue area of the oil painting *Victory Boogie Woogie* by Modriaan (1942–1944, Gemeentemuseum, Den Haag, Netherlands)—*grey line*—, *natural*, blue dress of A. Gaddi's mural painting. For all the spectra: C = calcite, Ox = oxalates, K = kaolin, B = organic binder

the Roman wall painting fragment. Examples of the features from surfaces painted with synthetic and natural ultramarine blue are shown in Fig. 9d. Synthetic ultramarine, on a blue area of the *Victory Boogie Woogie* by Mondriaan [38] shows the strong derivative band of Si–O stretching and the OH stretching of kaolin, whilst lapis lazuli, on a blue area of the mural painting by Agnolo Gaddi, exhibits the typical absorption of CO_2 at 2340 cm^{-1}.

4 Conclusion

Infrared spectroscopy, applied non-invasively through a fibre optic portable set-up, works in reflection mode acquiring both surface and volume reflection in a ratio that basically depends on the optical and morphological properties of the investigated material. Surface and volume reflections determine severe modifications of the spectral profile in comparison with the normal transmission mode spectrum (namely, inversion of bands, derivative shapes, changes of relative intensity). These modifications cannot be corrected by post processing algorithms, such us Kramers–Kronig and Kubelka–Munk, since the two reflection phenomena are coexisting. Nevertheless, knowing the reflection infrared properties of standard painting materials it is possible to define specific marker bands which, despite the spectral distortions, ensure a reliable identification of materials. In particular, for what is regarding inorganic pigments belonging to the classes of carbonates, sulphates and silicates, the fundamental bands generally used for their molecular identification in transmission mode measurements (namely, the antisymmetric stretching A–O, where A = C, S or Si) cannot be always considered in reflection spectra being strongly distorted by the *reststrahlen* effect, which is predominant for bands related to strong oscillators ($k \gg 1$). Conversely, combination and overtones of fundamentals are very good candidates as marker bands; in fact, having small absorption coefficients, these bands are at the same time not distorted by surface reflection and enhanced by volume reflection. The functional groups CO_3^{2-} and SO_4^{2-} exhibit combination and overtones of antisymmetric (ν_3) and symmetric stretching (ν_1) in the range 2600–1900 cm^{-1}, which are useful for the identification of their molecular structure, characterizing not only the type of cation (i.e. Pb, Cu, Ba, Ca, etc.) but also the hydration state. For the latter, combination and overtone bands of OH vibration modes can be also used to support the identification. Despite being not affected by reflection distortions, both combination and overtone bands fall in spectral ranges relatively free from possible overlappings with the other constituting materials, i.e. organic compounds as varnish, binders, etc. Although the organic infrared signals not interfere spectrally with the pigment identification, the presence of surface organic layers (varnish, coating) can generate such optically flat surfaces favouring surface reflection in spite of the diffuse one weakening and/or impeding the visualisation of the combination bands. Nevertheless, the exploiting of the NIR region of the overtone bands can allow for the identification of the pigment also when flat varnished surfaces are analysed.

The study of natural silicate pigments showed that also minor accessory minerals (such us quartz, kaolin or calcite) or impurities (i.e. carbon dioxide in lapis lazuli) can give clues for the pigment identification. In this regard is worth to underline that such minor phases are easily pinpointed in reflection mode thanks to the enhancement effect of diffuse reflection.

On the basis of the understanding gained studying the reflection infrared properties of reference pigments, the spectra acquired in situ on several case studies have been analysed and discussed. The successful results obtained on case studies ranging from wall paintings to manuscripts and from ancient to modern art, proved the strengths of reflection IR spectroscopy for the non-invasive molecular characterisation of pigments in complex and heterogeneous paint matrices.

Acknowledgements The work has been carried out through the support of the EU within the 6th FP (Contract Eu-ARTECH, RII3-CT-2004-506171) and the 7th FP (Contract CHARISMA nr. 228330).

References

1. M.R. Derrick, D. Stulik, J.M. Landry, *Infrared Spectroscopy* (Getty Conservation Institute, Los Angeles, 1999)
2. F. Casadio, L. Toniolo, J. Cult. Heritage **2**, 71 (2001)
3. R. Mazzeo, S. Prati, M. Quaranta, E. Joseph, E. Kendix, M. Galeotti, Anal. Bioanal. Chem. **392**, 65 (2008)
4. C. Miliani, F. Rosi, B.G. Brunetti, A. Sgamellotti, Acc. Chem. Res. **43**, 728 (2010)
5. http://www.eu-artech.org (last accessed 21/03/2011)
6. http://www.charismaproject.eu (last accessed 21/03/2011)
7. W.R. Scott, On site non destructive mid-IR spectroscopy of plastics in museum objects using a portable FT-IR spectrometer with fiber optics probe, in *Mat. Res. Soc. Symp., V*, December 3–5, Boston, Massachusetts, USA (1996)
8. R.S. Williams, in *The Sixth Infrared and Raman Users Group Conference,* Florence 2004, ed. by M. Picollo (Il Prato, Saonara, 2005), pp. 170–177
9. M. Fabbri, M. Picollo, S. Porcinai, M. Bacci, Appl. Spectrosc. **55**, 420 (2001)
10. M. Fabbri, M. Picollo, S. Porcinai, M. Bacci, Appl. Spectrosc. **55**, 428 (2001)
11. M. Bacci, M. Fabbri, M. Picollo, S. Porcinai, Anal. Chim. Acta **446**, 15 (2001)
12. F. Rosi, A. Daveri, C. Miliani, G. Verri, P. Benedetti, F. Piqué, B.G. Brunetti, A. Sgamellotti, Anal. Bioanal. Chem. **395**, 2097 (2009)
13. R. Ploeger, O. Chiantore, D. Scalarone, T. Poli, Appl. Spectrosc. **65**, 429 (2011)
14. T. Poli, O. Chiantore, M. Nervo, A. Piccirillo, Anal. Bioanal. Chem. doi:10.1007/s00216-011-4834-5 (2011)
15. C. Ricci, C. Miliani, B.G. Brunetti, A. Sgamellotti, Talanta **69**, 1221 (2006)
16. F. Rosi, A. Daveri, B. Doherty, S. Nazzareni, B.G. Brunetti, A. Sgamellotti, C. Miliani, Appl. Spectrosc. **64**, 956 (2010)
17. P. Griffiths, J.A. De Haseth, *Fourier Transform Infrared Spectrometry*, 2nd edn. (Wiley, New York, 2007)
18. E. Van Nimmen, K. De Clerck, I. Verschuren, K. Gellynck, T. Gheysens, J. Mertens, L. Van Langenhove, Vib. Spectrosc. **46**, 63 (2008)
19. M. Fox, *Optical Properties of Solids* (Oxford University Press, London, 2010)
20. M. Milosevic, S.L. Berets, Appl. Spectrosc. Rev. **37**, 347 (2002)
21. N. Eastaugh, V. Walsh, T. Chaplin, R. Siddall, *Pigment Compendium: A Dictionary and Optical Microscopy of Historic Pigments* (Elsevier, Amsterdam, 2008)
22. V.C. Farmer, *The Infrared Spectra of Minerals* (Mineralogical Society, London, 1974)
23. V. Chu, L. Regev, S. Weiner, E. Boaretto, Journal of Archaeological. Science **35**, 905 (2008)
24. M.E. Bottcher, P.L. Gehlken, D.F. Steele, Solid State Ion. **1379**, 101 (1997)
25. S. Gunasekaran, G. Anbalagan, S. Pandi, J. Raman Spectrosc. **37**, 892 (2006)
26. C. Haas, J.A.A. Ketelaar, Physica **22**, 1286 (1956)
27. M. Vagnini, C. Miliani, L. Cartechini, P. Rocchi, B.G. Brunetti, A. Sgamellotti, Anal. Bioanal. Chem. **395**, 2107 (2009)
28. F. Rosi, C. Miliani, A. Burnstock, B.G. Brunetti, A. Sgamellotti, Appl. Phys. A **89**, 849 (2007)
29. C. Miliani, F. Rosi, C. Ricci, A. Sassolini, F. Presciutti, C. Clementi, A. Sgamellotti, C. Seccaroni, P. Moioli, in *Proceedings of the Workshop "Raphael Painting Technique: Working Practice before Rome"*, London, England. Quaderni di Kermes (Nardini, Firenze, 2007)
30. F. Rosi, C. Miliani, C. Clementi, K. Kahrim, F. Presciutti, M. Vagnini, V. Manuali, A. Daveri, L. Cartechini, B.G. Brunetti, A. Sgamellotti, Appl. Phys. A **100**, 613 (2010)
31. C. Miliani, B. Doherty, A. Daveri, A. Loesch, H. Ulbricht, B.G. Brunetti, A. Sgamellotti, Spectrochim. Acta A-M **73**, 587 (2009)
32. C. Miliani, F. Rosi, I. Borgia, P. Benedetti, B.G. Brunetti, A. Sgamellotti, Appl. Spectrosc. **61**, 293 (2007)
33. C. Miliani, D. Buti, F. Presciutti, C. Clementi, A. Romani, A. Sgamellotti, D. Domenici, J. Arch. Sci. **39**(3), 672–679 (2012)
34. A. Duran, J. Castaing, P. Walter, Appl. Phys. A **99**, 333 (2010)
35. T.T. Nguyen, L.J. Janik, M. Raupach, Aust. J. Soil Res. **29**, 49 (1991)
36. F. Rosi, D. Daveri, A. Sgamellotti, B.G. Brunetti, C. Miliani, O.P.D. Quaderni (2011, in press)
37. F. Rosi, A. Burnstock, K.J. Van den Berg, C. Miliani, B.G. Brunetti, A. Sgamellotti, Spectrochim. Acta, A **71**, 1655 (2009)
38. C. Miliani, A. Sgamellotti, K. Kahrim, B.G. Brunetti, A. Aldrovandi, M.R. van Bommel, K.J. van den Berg, H. Janssen, *ICOM Committee for Conservation* (2008)
39. F. Rosi, C. Miliani, C. Clementi, K. Kahrim, F. Presciutti, M. Vagnini, V. Manuali, A. Daveri, L. Cartechini, B.G. Brunetti, A. Sgamellotti, Appl. Phys. A **100**, 613 (2010)
40. C. Miliani, V. Ciocan, A. Sgamellotti, B. Brunetti, in *Raffaello: La Rivelazione del Colore. Il Restauro Della Madonna del Cardellino* (Edifir, Firenze, 2009)
41. A. Daveri, C. Clementi, F. Presciutti, C. Anselmi, C. Miliani, A. Romani, B.G. Brunetti, A. Sgamellotti, in *L'ingegno e la Mano Restaurare il mai Restaurato* (Edifir, Firenze, 2009)
42. C. Miliani, A. Daveri, L. Spaabaek, A. Romani, V. Manuali, A. Sgamellotti, B.G. Brunetti, Appl. Phys. A **100**, 703 (2010)
43. J.J. Boon, K. Keune, M. Geldof, K. Mensch, S. Bryan, J.R.J. van Asperen de Boer, Chimia **55**, 952 (2001)
44. C. Miliani, A. Daveri, B.G. Brunetti, A. Sgamellotti, Chem. Phys. Lett. **466**, 148 (2008)
45. D. Bikiaris, S. Daniilia, S. Sotiropoulou, O. Katsimbiri, E. Pavlidou, A.P. Moutsatsou, Y. Chryssoulakis, Spectrochim. Acta, A **56**, 3 (1999)
46. http://www.irug.org/ed2k/search.asp (last accessed 21/03/2011)
47. R.L. Frost, U. Johansson, Clays Clay Miner. **46**, 466–477 (1998)

48. J. Madejová, P. Komadel, Clays Clay Miner. **49**, 410–432 (2001)
49. D. Hradil, T. Grygar, J. Hradilová, P. Bezdička, Appl. Clay Sci. **22**, 223 (2003)
50. F. Ospitali, D. Bersani, G. Di Lonardo, P.P. Lottici, J. Raman Spectrosc. **39**, 1066 (2008)
51. I. Aliatis, D. Bersani, E. Campani, A. Casoli, P.P. Lottici, S. Mantovana, I.G. Marino, F. Ospitali, Spectrochim. Acta A **73**, 532 (2009)
52. D. Hradil, A. Píšková, J. Hradilová, P. Bezdička, G. Lehrberger, S. Gerzer, Archaeometry (2010). doi:10.1111/j.1475-4754.2010.00554.x
53. M. Bacci, M. Picollo, Stud. Conserv. **41**, 136 (1996)
54. G.A. Mazzocchin, F. Agnolia, M. Salvadori, Talanta **64**, 732 (2004)
55. I. Hassan, R.C. Peterson, H.D. Grundy, Acta Crystallogr. C **41**, 827 (1985)